

tophagy factor, Atg7. Atg7 inhibition by siRNA (Fig. 3C) resulted in a decrease of IFN- γ -induced LC3 puncta in U937 cells (Fig. 3B and fig. S6A). In U937 cells treated with hIFN- γ and then transfected with either IRGM or control (scrambled) siRNA, the hIFN- γ -dependent increase in GFP-LC3 puncta was not affected in cells transfected with the control (scrambled) siRNA (Fig. 3D and fig. S6B). However, when cells were transfected with IRGM siRNA, the number of GFP-LC3 puncta decreased relative to that of the control cells (Fig. 3D and fig. S6B).

The role of IRGM in the conversion of endogenous LC3-I into the LC3-II form in human macrophages was confirmed by immunoblotting. IRGM inhibition by siRNA specifically reduced the amounts of LC3-II in cells treated with hIFN- γ (Fig. 3E). Moreover, when autophagy was induced with the conventional inducer rapamycin, IRGM siRNA inhibited the formation of LC3-II (Fig. 3E). Thus, IRGM is necessary for the execution of the autophagic pathway in human macrophages.

To determine whether human IRGM is involved in the resistance to mycobacteria in a manner similar to that of Irgm1 in murine cells (4), we examined the status of mycobacterial phagosomes. U937 cells were transfected with either control siRNA or IRGM siRNA, and autophagy was induced by starvation. Acidification of mycobacterial phagosomes was monitored by LT staining (Fig. 4, A and B). The proportion of mycobacterial phagosomes that tested positive for LT increased (50.6%) upon starvation as compared with the control cells (21%) ($P < 0.01$). In contrast, cells transfected with IRGM siRNA showed only 28% of LT colocalization with mycobacterial phagosomes upon induction of autophagy by starvation (Fig. 4, A and B). Thus, not only does IRGM participate in autophagy in human macrophages, but IRGM-dependent processes are also required for autophagy-induced BCG phagosome maturation in human cells. To test whether IRGM affects mycobacterial survival in human macrophages, we transfected human U937 cells with either control siRNA or IRGM siRNA, infected them with mycobacteria, and examined bacterial viability by counting colony-forming units in a time-course experiment after infection. Increased bacterial survival was observed in cells that were treated with IRGM siRNA compared to that in control cells (Fig. 4C). Thus, IRGM, the human ortholog of Irgm1 (LRG-47), acts as its functional equivalent in autophagy and plays a role in the control of intracellular mycobacteria in human cells.

IFN- γ induces multiple microbicidal pathways, with IRG (2, 3) and autophagy (7) representing two of its effectors linked together in this work. The Irgm1-induced organelles represent autophagosomes and autolysosomes that are in transit through various stages of development, with terminal vacuoles that are much larger than conventional autolysosomes. Thus, Irgm1-stimulated processes allow for enhanced

growth of individual autophagic organelles and may be important for efficient capture of geometrically challenging pathogens, such as clumps of *M. tuberculosis* (movie S1). Unlike the IRG family in mice, the human IRGM is not responsive to IFN- γ and is constitutively expressed (1). Nevertheless, IRGM participates in IFN- γ -induced or conventionally induced (by rapamycin or starvation) autophagy in human macrophages, indicating a more general role for IRGM in autophagy. IRGM participates in conferring resistance against mycobacterial infections, fulfilling a role analogous to that of Irgm1 in mice. In conclusion, this study demonstrates a role for the IRG proteins in autophagy, thereby uncovering the mechanism of action by which this class of host defense factors confers resistance to intracellular pathogens.

References and Notes

1. C. Bekpen *et al.*, *Genome Biol.* **6**, R92 (2005).
2. G. A. Taylor, C. G. Feng, A. Sher, *Nat. Rev. Immunol.* **4**, 100 (2004).
3. J. D. MacMicking, *Curr. Opin. Microbiol.* **8**, 74 (2005).
4. J. D. MacMicking, G. A. Taylor, J. D. McKinney, *Science* **302**, 654 (2003).
5. S. Martens *et al.*, *PLoS Pathog.* **1**, e24 (2005).
6. C. G. Feng *et al.*, *J. Immunol.* **172**, 1163 (2004).
7. M. G. Gutierrez *et al.*, *Cell* **119**, 753 (2004).
8. T. Shintani, D. J. Klionsky, *Science* **306**, 990 (2004).
9. I. Nakagawa *et al.*, *Science* **306**, 1037 (2004).
10. M. Ogawa *et al.*, *Science* **307**, 727 (2005).

11. C. Paludan *et al.*, *Science* **307**, 593 (2005).
12. C. L. Birmingham, A. C. Smith, M. A. Bakowski, T. Yoshimori, J. H. Brummel, *J. Biol. Chem.* **281**, 11374 (2006).
13. V. Deretic, *Trends Immunol.* **26**, 523 (2005).
14. B. Levine, *Cell* **120**, 159 (2005).
15. V. Deretic, Ed. *Autophagy in Immunity and Infection* (Wiley-VCH, Weinheim, Germany, 2006).
16. Y. Liu *et al.*, *Cell* **121**, 567 (2005).
17. S. P. Elmore, T. Qian, S. F. Grissom, J. J. Lemasters, *FASEB J.* **15**, 2286 (2001).
18. P. O. Seglen, P. B. Gordon, I. Holen, *Semin. Cell Biol.* **1**, 441 (1990).
19. Y. Kabeya *et al.*, *EMBO J.* **19**, 5720 (2000).
20. X. H. Liang *et al.*, *Nature* **402**, 672 (1999).
21. A. Kihara, Y. Kabeya, Y. Ohsumi, T. Yoshimori, *EMBO Rep.* **2**, 330 (2001).
22. N. Furuya, J. Yu, M. Byfield, S. Pattingre, B. Levine, *Autophagy* **1**, 46 (2005).
23. X. Zeng, J. H. Overmeyer, W. A. Maitese, *J. Cell Sci.* **119**, 259 (2006).
24. We thank T. Ueno and E. Kominami for the LC3 antibody, E. Roberts for experimental input, and G. Timmins for comments. This work was supported by grants from the National Institute of Allergy and Infectious Diseases (AI57831 to G.A.T.; AI45148 and AI42999 to V.D.).

Supporting Online Material

www.sciencemag.org/cgi/content/full/1129577/DC1
Materials and Methods

Figs. S1 to S6

References

Movie S1

5 May 2006; accepted 25 July 2006

Published online 3 August 2006;

10.1126/science.1129577

Include this information when citing this paper.

Humanization of Yeast to Produce Complex Terminally Sialylated Glycoproteins

Stephen R. Hamilton,¹ Robert C. Davidson,¹ Natarajan Sethuraman,¹ Juergen H. Nett,¹ Youwei Jiang,¹ Sandra Rios,¹ Piotr Bobrowicz,¹ Terrance A. Stadheim,¹ Huijuan Li,¹ Byung-Kwon Choi,¹ Daniel Hopkins,¹ Harry Wischnewski,¹ Jessica Roser,¹ Teresa Mitchell,¹ Rendall R. Strawbridge,² Jack Hoopes,² Stefan Wildt,¹ Tillman U. Gerngross^{1,3*}

Yeast is a widely used recombinant protein expression system. We expanded its utility by engineering the yeast *Pichia pastoris* to secrete human glycoproteins with fully complex terminally sialylated N-glycans. After the knockout of four genes to eliminate yeast-specific glycosylation, we introduced 14 heterologous genes, allowing us to replicate the sequential steps of human glycosylation. The reported cell lines produce complex glycoproteins with greater than 90% terminal sialylation. Finally, to demonstrate the utility of these yeast strains, functional recombinant erythropoietin was produced.

The half-life and therapeutic potency of most glycoproteins, with the notable exception of antibodies, is dependent on the presence of terminal sialic acid. The ex-

posure of other terminal sugars such as mannose, N-acetylglucosamine, and galactose on a glycoprotein leads to clearance by sugar-specific receptors or lectins (1, 2). Because most therapeutic glycoproteins require sialylation, their production to date has relied on mammalian hosts, which are able to perform humanlike N-glycosylation, including the ability to add terminal sialic acid. Yeast and filamentous fungi offer numerous advantages as recombinant protein expression systems when compared with mammalian cell culture, including higher recombinant protein titers,

¹GlycoFi Inc., 21 Lafayette Street, Suite 200, Lebanon, NH 03766, USA. ²Department of Surgery, Dartmouth-Hitchcock Medical Center, Lebanon, NH 03766, USA. ³Thayer School of Engineering, Department of Biological Sciences and Department of Chemistry, Dartmouth College, 8000 Cummings Hall, Hanover, NH 03755, USA.

*To whom correspondence should be addressed. E-mail: tillman.gerngross@dartmouth.edu

shorter fermentation times, and the ability to grow in chemically defined media. However, wild-type yeast glycosylate proteins with high-mannose type N-glycans (3) (Fig. 1A), which reduce half-life and compromise therapeutic function. Our laboratory has been engineering human glycosylation pathways into fungal hosts, including the yeast *P. pastoris* (4–6). The core repertoire of human glycosylation reactions (Fig. 1A) requires the sequential removal of mannose by two distinct mannosidases (i.e., α -1,2-mannosidase and manno-

sidase II), the addition of *N*-acetylglucosamine (by *N*-acetylglucosaminyltransferase I and II), the addition of galactose (by β -1,4-galactosyltransferase), and finally the addition of sialic acid by sialyltransferase. Sialylation, the final step of human glycosylation, is particularly difficult to accomplish in yeast, because wild-type yeast lacks all four prerequisites: (i) the ability to produce the *N*-glycosylated precursors terminating in β -1,4-galactose, (ii) the biosynthetic capability to produce the sugar nucleotide pre-

cursor cytidine monophosphate (CMP)-sialic acid [specifically, CMP-*N*-acetylneuraminic acid (CMP-NANA)], (iii) the transporter to shuttle CMP-sialic acid into the Golgi, and (iv) a sialyltransferase to transfer sialic acid to terminal galactose on the nascent glycoprotein (fig. S1) (7). All of these elements must work at high efficiency to allow for the production of sialylated glycoproteins, and organelle-specific targeting of several elements is required to permit these functions to occur in concert.

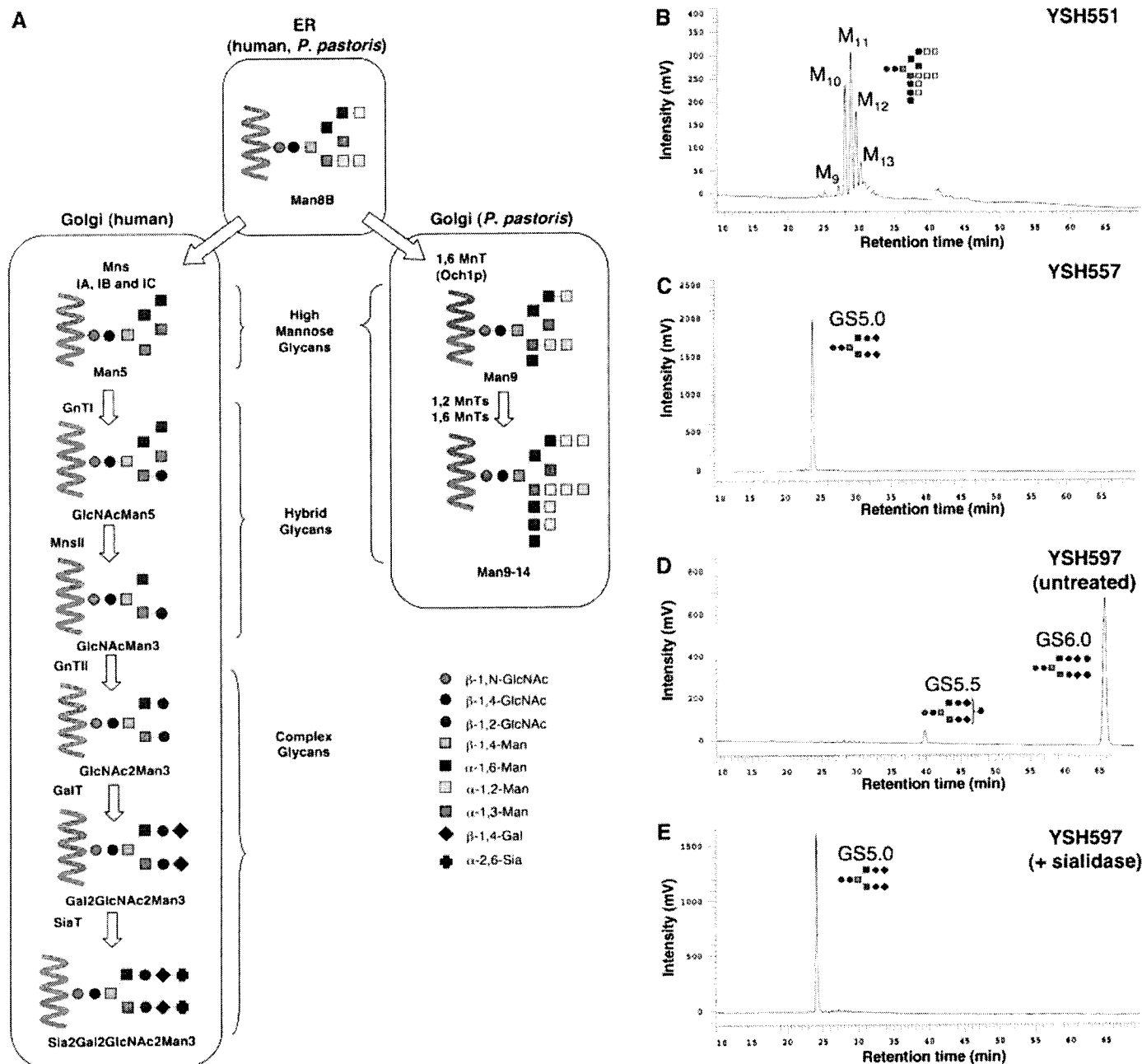


Fig. 1. N-linked glycosylation pathways and characterization of N-linked glycans released from recombinant rEPO. (A) Representative N-linked glycosylation pathways in humans and *P. pastoris*. Mns: α 1,2- mannosidase; MnsII: mannosidase II; GnTI: β 1,2-*N*-acetylglucosaminyltransferase I; GnTII: β 1,2-*N*-acetylglucosaminyltransferase II; GalT: β 1,4-galactosyltransferase; SiaT: α 2,6-sialyltransferase; MnT: mannosyltransferase. (B to D) rEPO secreted from

P. pastoris strains YSH551 (B), YSH557 (C), and YSH597 (D) was purified from culture supernatants by Ni-affinity chromatography. Glycans were released by PNGase-F treatment and labeled with 2-AB before HPLC analysis. (E) Glycans secreted from YSH597 containing sialic acid were treated with α -2,3-/2,6-/2,8-sialidase. Elution times for commercial glycan standards corresponding to GS5.0, 5.5, and 6.0 were 24, 40, and 66 min, respectively.

Erythropoietin (EPO) is a hematopoietic glycoprotein that stimulates the differentiation of late erythroid progenitor cells to mature red blood cells (8). Since a recombinant source of the protein has become available, EPO has found wide therapeutic use in the treatment of anemia. EPO is a heavily glycosylated protein, with three N-glycosylation sites and up to 40% of the molecular mass attributable to its glycans (9, 10). As with many glycoproteins, the therapeutic efficacy and receptor affinity of EPO relies on the degree and composition of N-glycosylation (11).

A previously reported glycoengineered strain of *P. pastoris* produces terminally galactosylated biantennary glycans of the complex type Gal₂GlcNAc₂Man₃GlcNAc₂ (i.e., Glycan Structure 5.0, GS5.0) (12). This strain RDP750 [*Δoch1*, *Δpno1*, *Δmnn4B*, *Δbmu2*, *Δhis1*, *Kluyveromyces lactis* and *Mus musculus* uridine diphosphate (UDP)-GlcNAc transporters, *Mus musculus* α-1,2-MnsI, *Homo sapiens* β-1,2-GlcNAc transferase I, *Rattus norvegicus* β-1,2-GlcNAc transferase II, *Drosophila melanogaster* MnsII, *Schizosaccharomyces pombe* Gal epimerase, *D. melanogaster* UDP-Gal transporter, and *H. sapiens* β-1,4-galactosyltransferase] was transformed with an expression plasmid encoding for rat EPO (rEPO) to generate strains RDP762 and YSH557 (7). Secreted rEPO from YSH557 consisted predominantly of GS5.0 N-glycans (Fig. 1C). For comparison, the same construct was used to transform wild-type *P. pastoris* NRRL-Y11430, resulting in strain YSH551, which secreted rEPO with mostly high-mannose N-glycans that are typical for this yeast (3) (Fig. 1B). Both strains displayed similar growth characteristics and expressed rEPO at about the same level (~20 mg/liter), although the proteins differed significantly with respect to their N-glycosylation (Fig. 1, B and C).

To accomplish the final step of human glycosylation, the addition of terminal sialic acid, we transformed *P. pastoris* strain RDP762 with a range of DNA constructs encoding for enzymes involved in CMP-sialic acid biosynthesis, CMP-sialic acid transport, and sialic acid transfer to the

nascent glycoprotein. In total, five enzymes were selected: *H. sapiens* UDP-N-acetylglucosamine-2-epimerase/N-acetylmannosamine kinase (GNE), *H. sapiens* N-acetylneuraminase-9-phosphate synthase (SPS), *H. sapiens* CMP-sialic acid synthase (CSS), *M. musculus* CMP-sialic acid transporter (CST), and a library of chimeric sialyltransferases linked to yeast type-II transmembrane localization peptides (ST).

More than 120 permutations of alternative CMP-sialic acid pathways, CSTs, and STs were screened. From this screen, we identified a small number of combinations displaying significant sialyltransferase activity and producing predominantly complex glycan structures. However, taking this approach we were unable to obtain glycan compositions containing >60% GS6.0 (Sia₂Gal₂GlcNAc₂Man₃GlcNAc₂).

To further improve the efficiency of sialylation, we codon-optimized GNE, SPS, CSS, and CST, and screened additional ST/leader fusions. The catalytic domain of mouse α-2,6-ST, fused to the *Saccharomyces cerevisiae* mannosyltransferase 1 (Mnt1) targeting signal was particularly effective. To consolidate these efforts, we cloned all five genes into a single expression vector, pSH926 (7). Transformation of this vector into RDP762 complemented the histidine auxotrophy of the host, while targeting the gene cluster to the *TRP2* locus of the *Pichia* genome. The resulting strain, designated YSH597, was cultured in shake flasks to secrete rEPO. Analysis of the N-glycans isolated from rEPO displayed a glycan composition that consisted predominantly of sialylated glycan structures GS6.0 (90.5%) and GS5.5 (7.9%, SiaGal₂GlcNAc₂Man₃GlcNAc₂) (Fig. 1D). Subsequent treatment of this sample with sialidase showed quantitative conversion to GS5.0 (Fig. 1E), confirming that GS6.0 and GS5.5 were terminally sialylated glycans.

To assess the activity of these two different rEPO glycoforms in vivo, we purified material from wild-type *P. pastoris* (YSH551) and YSH597 (7). The purified protein was characterized by sodium dodecyl sulfate-polyacrylamide gel elec-

trophoresis (SDS-PAGE) (Fig. 2A), and rEPO from wild-type *P. pastoris* showed extensive heterogeneity consistent with hyperglycosylation and the range of high-mannose structures found by high-performance liquid chromatography (HPLC) (Fig. 1B). In contrast, rEPO from YSH597 showed a more uniform migration pattern, consistent with the glycan uniformity found by HPLC (Fig. 1D). As expected, when both samples were treated with peptide N-glycosidase F (PNGase-F), to remove the N-glycans, the mass and uniformity of the deglycosylated material appeared similar (Fig. 2A). To compare the functionality of these two vastly different glycoforms, animal studies were performed to determine their respective erythropoietic function. As expected, rEPO produced in wild-type yeast had no measurable erythropoietic function, whereas rEPO produced in YSH597 showed a dose-dependent response consistent with a biologically active form of the protein (Fig. 2B).

We report the generation of yeast cell lines of *P. pastoris* with a substantially reengineered secretory pathway. These cell lines secrete terminally sialylated, complex, bi-antennary glycoproteins as exemplified by rEPO, as well as other recombinant proteins tested. The availability of such yeast cell lines may eliminate the need for mammalian cell culture in the future and allow for the production of therapeutic glycoproteins in a nonmammalian host. While significantly reducing production time and viral containment issues, this will also provide improvements in product uniformity and overall production economics. Previously, a panel of glycoengineered yeast cell lines displaying a limited repertoire of human glycosylation reactions allowed us to elucidate glycosylation-dependent structure activity relationships (12). Here, we have engineered into yeast the most complex step of human N-glycosylation, terminal sialylation, which will expand our ability to conduct structure-function investigations.

References and Notes

1. G. Ashwell, J. Harford, *Annu. Rev. Biochem.* **51**, 531 (1982).
2. R. J. Stockert, *Physiol. Rev.* **75**, 591 (1995).
3. I. R. Gemmill, R. B. Trimble, *Biochim. Biophys. Acta* **1426**, 227 (1999).
4. B. K. Choi *et al.*, *Proc. Natl. Acad. Sci. U.S.A.* **100**, 5022 (2003).
5. S. R. Hamilton *et al.*, *Science* **301**, 1244 (2003).
6. P. Bobrowicz *et al.*, *Glycobiology* **14**, 757 (2004).
7. Materials and methods are available as supporting material on Science Online.
8. J. L. Spivak, *Blood Rev.* **3**, 130 (1989).
9. P. H. Lai, R. Everett, F. F. Wang, T. Arakawa, E. Goldwasser, *J. Biol. Chem.* **261**, 3116 (1986).
10. J. M. Davis, T. Arakawa, T. W. Strickland, D. A. Yphantis, *Biochemistry* **26**, 2633 (1987).
11. M. N. Fukuda, H. Sasaki, L. Lopez, M. Fukuda, *Blood* **73**, 84 (1989).
12. H. Li *et al.*, *Nat. Biotechnol.* **24**, 210 (2006).
13. We thank A. Kull, H. Lynaugh, and A. Thompson for their technical assistance. T.U.G. is a founder of GlycoFi and has equity holdings in Merck. GlycoFi is a wholly owned subsidiary of Merck as of 6 June 2006.

Supporting Online Material

www.sciencemag.org/cgi/content/full/313/5792/1441/DC1
Materials and Methods
Figs. S1 and S2
References

22 May 2006; accepted 4 July 2006
10.1126/science.1130256

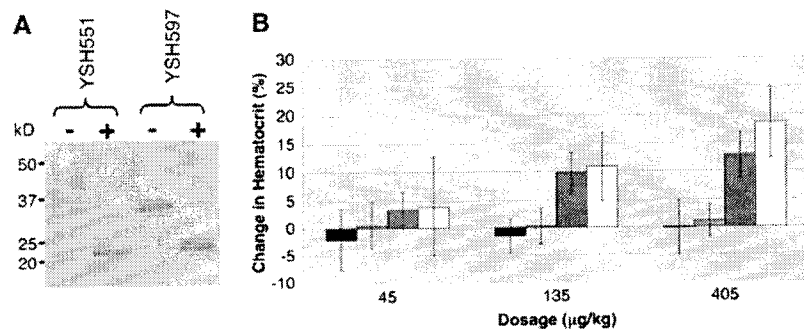


Fig. 2. Characterization of recombinant rEPO obtained from *P. pastoris*. (A) SDS-PAGE analysis of recombinant rEPO (2.5 µg, postpurification) secreted from YSH551 and YSH597 strains after incubation in the presence (+) or absence (−) of PNGase-F. (B) Comparative hematocrit analysis of recombinant rEPO secreted from YSH551 (blue and green bars) and YSH597 (red and yellow bars). Values correspond to days 8 (blue and red bars) and 15 (green and yellow bars) after initial injection. Data presented as mean ± SD of *n* = 5 mice per dose.